Heart Surgery Forum 2023; 26(4): E390–E407
doi: 10.59958/hsf.5925

Article

Unveiling Immune-Metabolic Interaction in Atherosclerosis via Comprehensive Landscape of Hub Genes and Immune Microenvironment

Fang Liu[1,2,*], Tao Li[3], Xiuwen Liu[1], Demeng Qin[1]

[1]International Genome Center, Jiangsu University, 212013 Zhenjiang, Jiangsu, China
[2]Department of Vascular Surgery, Affiliated Hospital of Jiangsu University, 212001 Zhenjiang, Jiangsu, China
[3]Department of Information, Jianbi Community Healthcare Center, 212006 Zhenjiang, Jiangsu, China
*Correspondence: liuujs2021@163.com (Fang Liu)

Submitted: 3 July 2023 Revised: 19 August 2023 Accepted: 22 August 2023 Published: 28 August 2023

Abstract

Objective: Atherosclerosis (AS) as a major cause of cardiovascular diseases, is considered a chronic inflammatory disease and accelerates by inflammation, lipid metabolism disorder and other mechanisms. AS pathogenesis and its relationship with immune regulation and metabolic interactions is still not fully elucidated. The purpose of this study is to delve into the correlation between mitochondrial metabolism and immunity in AS, and identify potential therapeutic targets for clinical treatment. **Methods**: Hub genes associated with mitochondrial metabolism and the pathogenesis of AS were identified by performing differentially expressed genes (DEGs) analysis and Weighted Gene Co-expression Network Analysis (WGCNA) based on two gene expression datasets (GSE100927 and GSE43292). And the biological processes and pathways of DEGs were determined through gene ontology (GO) and Gene Set Enrichment Analysis (GSEA) analysis. Then stepwise regression, random forest, and Lasso regression machine learning were used to evaluate the diagnostic value of hub genes. After that, the immune infiltration and single cell sequencing dataset GSE184073 were analyzed, and the immune cell composition in peripheral blood from AS patients using Mass Cytometry were detected to further consider the influence of immunoregulation. **Results**: Ten hub genes associated with mitochondrial metabolism and AS pathogenesis were identified, including *NDUFS4*, *AIFM3*, *IDUA*, *TNF*, *CHKA*, *SLC11A1*, *SLC35C1*, *SLC37A2*, *ARSB*, *SLC16A5*. GO and GSEA analysis showed their correlation with immunity and inflammation. Lasso regression revealed that *TNF* and *ARSB* had relatively good diagnostic performance. Further exploration was conducted on the expression of these hub genes in the immune microenvironment and their correlation with different immune factors. Mass cytometry demonstrated the influence of the vascular immune microenvironment on the pathogenesis of AS. **Conclusions**: Our study provides a more comprehensive understanding of the complex relationships between immune and metabolic factors and their impact on the microenvironment of AS. The identification of hub genes in AS may provide new targets for therapeutic intervention.

Keywords

atherosclerosis; hub genes; immunoregulatory; metabolism

Introduction

A significant number of deaths and disabilities worldwide are caused by cardiovascular diseases, which significantly impact health and quality of life. Atherosclerosis (AS), the underlying disorder in many cardiovascular conditions such as stroke, heart disease and peripheral vascular diseases, is conventionally believed to be initiated and progress due to chronic inflammation [1,2]. However, recent advancements in our understanding of AS pathogenesis, treatment and prognosis assessment have revealed its complex nature, highlighting the pivotal role of immune regulation and the metabolic microenvironment [3,4]. Previously, AS was primarily attributed to the gradual buildup of cholesterol, particularly low-density lipoprotein (LDL), within the arterial walls. Following oxidative modification, the retained LDL in the arterial wall is captured by scavenger receptors and phagocytosed by infiltrated macrophages, leading to the formation of foam cells [5]. Currently, available therapies for AS in clinical practice mainly focus on medications that lower plasma lipid and LDL cholesterol levels while increasing high-density lipoprotein cholesterol [6]. Thus, AS must be diagnosed and treated with the use of new molecules.

The pathogenesis of AS is thought to involve proinflammatory and immune signaling pathways, oxidative stress, and mitochondrial dysfunction. Inflammation and metabolic processes are key factors in the development of atherosclerotic plaques [7,8]. In the early stages of AS, in response to vascular endothelial damage, leukocytes are recruited and proinflammatory cytokines are released. Metabolic abnormalities contribute to the accumulation of surplus lipids, which are stored as cholesteryl esters and triglycerides in lipid droplets [9]. After lipoprotein particles are engulfed by monocytes/macrophages through scavenger receptors, foam cells form and result in atheroscle-

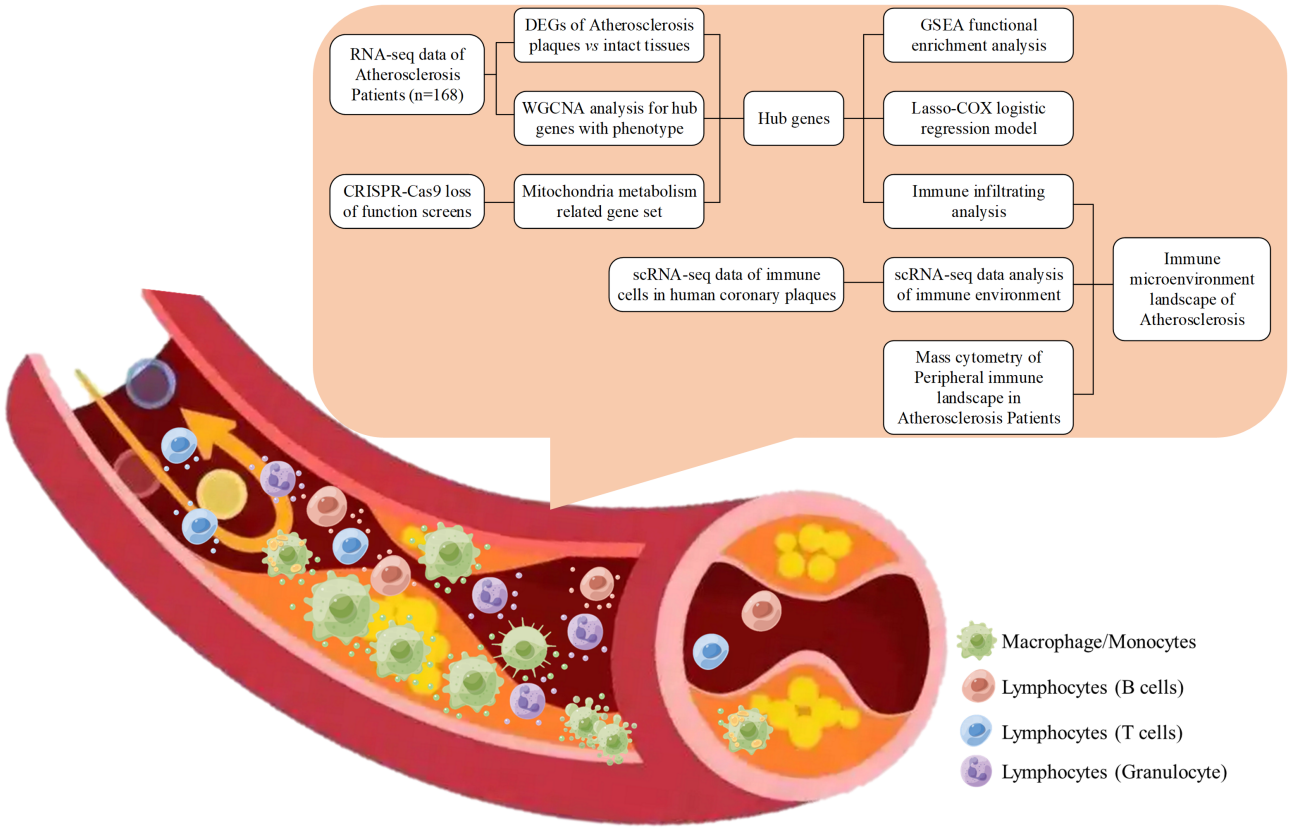

Graphical Abstract

rotic plaque formation [10]. As the plaques progress, the apoptosis and necrosis of foam cells and intraplaque hemorrhage further reduce viscosity and ultimately lead to thrombotic obstruction of arteries [11,12]. Mitochondria are important in lipid metabolism and accumulation due to their function in oxidizing fatty acids and synthesizing lipids [13,14].

Additionally, the pathophysiology of AS appears to be influenced by abnormal immune regulation, as well as abnormal metabolism. It has been observed that both adaptive and innate immune responses are involved in the development of AS [15]. Innate immunity relies primarily on macrophages and cytokines, while adaptive immune responses contribute to AS progression and plaque instability [16]. T cells are mainly engaged in aggravating atherogenesis, which receives inhibitory signals from T-helper 2 and regulatory T cells [17,18]. B cells also play a dual role in AS, as they exert proatherogenic activities, while natural IgM antibodies derived from B1 cells demonstrate antiatherogenic properties [19]. The intricate relationship between inflammation, immunity, and intermediate metabolism has emerged as an area of significant interest in AS research. Thus, given the crucial role of inflammation in AS, it is important to understand the interaction between immunological and metabolic factors interact to shed light on how these factors collectively contribute to the alteration of the disease.

This study aims to identify hub genes associated with the pathogenesis of AS and mitochondrial metabolism. To achieve this, we performed differential analysis and utilized the Weighted Gene Co-Expression Network Analysis (WGCNA) approach on two gene expression datasets (GSE100927 and GSE43292). Then, Gene Ontology (GO) and Gene Set Enrichment Analysis (GSEA) were performed to identify the relevant biological processes and pathways. To assess the diagnostic value of these hub genes, stepwise regression, random forest and least absolute shrinkage and selection operator (LASSO) regression machine learning algorithms were employed, demonstrating relatively good diagnostic performance based on the area under the curve (AUC) values and indicating the promising clinical application of the identified hub genes in diagnosing AS. In order to investigate the immunoregulatory influence of these hub genes, immune factors and the infiltration of these samples were examined. The immune microenvironment landscape in acute and stable AS plaques was explored using the single-cell sequencing dataset GSE184073, allowing for the analysis of hub gene expression in various immune cell subpopulations. Additionally, Mass Cytometry was performed to validate the immune cell composition in peripheral blood from AS patients, and multi-dimensional analyses of the immune cell composition were conducted to enhance the understanding of this complex disease process. Overall, this study contributes to identifying hub genes in AS, providing new

insights into their biology, a more comprehensive understanding of the intricate relationships between immune and metabolic factors and their impact on the microenvironment of AS, and their potential as therapeutic targets.

Materials and Methods

Data Acquisition

Raw gene expression profiles for GSE100927 and GSE43292 were extracted from NCBI's Gene Expression Omnibus (GEO) database (https://www.ncbi.nlm.nih.gov/geo/). The GSE100927 dataset comprises 69 samples from the atherosclerotic carotid artery and 35 control samples from individuals without atherosclerotic lesions (collected from deceased organ donors). Based on the GPL17077 platform, gene expression data was detected (Agilent-039494 SurePrint G3 Human GE v2 8x60K Microarray). In the GSE43292 dataset, samples were collected from 32 hypertensive patients, consisting of their atheroma plaques and distant macroscopically intact tissues, which were detected by the GPL6244 platform (Affymetrix Human Gene 1.0 ST Array).

Data Pre-Processing

The "SilicoMerging" package was used to merge and pre-process the raw gene expression data from the two gene expression matrices, crucial for extracting relevant information from the datasets [20]. Then, the expression values were corrected for batch effects using COMBAT [21], and the probe ID for every gene was converted to its corresponding gene symbol using a Perl script.

Differential Expression Analysis

Differential expression analysis of genes (DEGs) between atherosclerosis and normal samples was conducted using the "limma" package in the R software (version 4.2.2; Development Core Team, Auckland, New Zealand). Genes with a p-value < 0.05, False Discovery Rate (FDR) <0.05 and an absolute log fold change (logFC) >1.2 were considered DEGs. Volcano plots and heat maps depicting the DEGs were generated using the "ggplot2" R package.

Weighted Correlation Network Analysis (WGCNA)

A gene-phenotype relationship was explored using the WGCNA package in R. A median absolute deviation (MAD) for each gene was calculated using gene expression profiles, and genes with lower MAD values (50%) were removed. Pearson's correlation analysis was then performed to cluster the samples and detect outliers. The WGCNA package was then used to construct a scale-free co-expression network. This involved creating a Pearson's correlation matrix and applying the average linkage method to pair-wise genes. A weighted adjacency matrix was generated using a power function ($a_{mn} = |c_{mn}|^{\beta}$) to emphasize strong gene correlations and penalize weak ones. The power value (β) of 14 was selected, and the adjacency matrix was transformed into a topological overlap matrix (TOM) to measure gene network connectivity. The dissimilarity (1-TOM) was calculated. To identify gene modules with similar expression profiles, average linkage hierarchical clustering was performed based on TOM-based dissimilarity, with a minimum module size of 30 genes and a sensitivity set at 3. Module eigengenes were used to calculate dissimilarity and determine module dendrograms. Modules with a distance less than 0.25 were merged, resulting in 9 modules. The grey module represents genes that could not be assigned to a specific module and lack reference significance. Finally, module membership (MM) was calculated to assess the importance of genes within each module by measuring the correlation between module eigenvectors and individual gene expression. Based on a threshold of $|c_{mn}| >0.8$, 71 hub genes with high connectivity were identified within the clinically significant brown module. The soft threshold power was assessed, and a value of 14 was chosen as it resulted in the successful construction of scale-free networks with an independence degree of up to 0.870 and an average connectivity of 0.626. Using a merging threshold of 0.25 and a minimum module size of 30, a total of 9 distinct co-expression modules were identified through dynamic tree cutting.

Metabolism-Related Genes

Metabolism-related gene sets, encompassing 2977 genes associated with small molecule transporters involved in metabolism, as well as metabolism-related transcription factors, were extracted from genome-wide CRISPR-Cas9 loss-of-function screens, emphasizing the pivotal role of mitochondria in metabolic processes [22,23] (**Supplementary Table 1**).

Identification of Hub Genes

The "VennDiagram" R package was used to determine the crossroads of DEGs, hub genes obtained through WGCNA analysis, and genes from the metabolism-related gene sets, aiming to identify hub genes associated with both mitochondria-related metabolism and AS. A violin plot was used to display the differential expression of hub genes between the AS and NA group. The statistical significance of the differential expression was assessed using hypothesis tests, and the significance level was set at p-value < 0.01 for both the t-test and Mann-Whitney U-test.

Quantitative RT-PCR (qRT-PCR)

In order to further confirmed the expression of hub genes in AS lesion and normal tissues, we isolated total ri-

bonucleic acid (RNA) of five patients AS plaques and their distant macroscopically intact tissues using the TRIZOL reagent (Invitrogen, Shanghai, China). Subsequently, the complementary DeoxyriboNucleic Acid (cDNA) was synthesized using the High Capacity cDNA Reverse Transcription kit (AE311-02; Transgene, Beijing, China) and then amplified employing the SYBR Green master mix (AQ131-01; Transgene, Beijing, China) on a QuantStudio3 system (Thermo Fisher Scientific, MA, USA). The internal control used was β-actin. The relative quantification of gene expression was determined with respect to β-actin levels. The primer sequences are provided below:

Ndufs4: TGCTCGCAATAACATGCAGTC, GATCAGCCGTTGATGCCCAA;

Aifm3: CTGTCTGCCACGTCAAGGAC, GCCGTAGTGCGGACACTTAT;

Idua: CAGGAGATACATCGGTAGGTACG, TCATGGAGACGTTGTCAAAGTC;

Tnf: GAGGCCAAGCCCTGGTATG, CGGGCCGATTGATCTCAGC;

Chka: TGGTTCTGGAGAGCGTTATGT, CATTTTCTCGGCGATTTCTGC;

Slc11a1: ACAAGGGTCCCCAAAGGCTA, CACTCAGGTAGGTCTCTCTGG;

Slc35c1: CTGCCTCAAGTACGTCGGTG, CCGATGATGATACCGCAGGTG;

Slc37a2: CCGGGAGTCTGGTTCTTCC, ACGATACTGATAGGCTTCCTGG;

Arsb: TCTTGCTGGCAGACGACCTA, GGCTGCGTGTAGTAGTTGTCC;

Slc16a5: TCAGCCAGCTCTACTTCACAG, CGCCGAAGACAAGGAAGGT.

Functional Enrichment Analysis

A functional enrichment analysis was conducted to elucidate the biological mechanisms by which the hub genes influence AD. GO analyzed these genes based on their biological processes, cellular components, and molecular functions. Then, GSEA was performed to reveal the specific functions of each gene. Next, the samples were categorized into two groups based on the median expression levels of the hub genes: the low-expression group and the high-expression group. The C2 collection, which consists of 4850 curated gene sets from the Molecular Signature Database (MsigDB) [24], was used for pathway enrichment analysis. GSEA was performed using the following parameters: 1000 permutations, 'Collapse data set' set to FALSE, permutation type set to gene_set, max size set to 5000, and min size set to 1. The functional enrichment analysis results were visualized using the "Enrichplot" R package. All analyses were performed using the "ClusterProfiler" R package.

Logistic Regression Model

The Lasso-COX logistic regression model was used to evaluate the accuracy of the hub genes in predicting disease diagnosis. We integrated clinical characteristics with the expression levels of the 10 hub genes using the Survival package in R. We estimated the prevalence of the 10 hub genes using a COX proportional hazards regression analysis. The C-index was determined to be 0.9278, and the hazard ratios and their corresponding 95% confidence intervals were plotted using the "Forestplot" R package. Then, the "pROC" R package was used to perform ROC curve analysis, which involved calculating the area under the ROC curve (AUC). DeLong's test was performed using all z-normalized scores for all studies combined [25].

Immune Cell Infiltration and Immunological Function Analysis

The fractions of multiple cell types within gene expression profiles of admixtures were predicted by CIBERSORT, a deconvolution algorithm based on gene expression. Here, CIBERSORT was used to assess immune cell infiltration in the microenvironment, employing 547 biomarkers and 22 human immune cells. The gene composition of each sample was determined by analyzing the expression levels of individual genes in relation to the composition and proportion of the 22 immune cell types across the 168 samples. Subsequently, Spearman correlation analysis was conducted to explore the relationships between the identified hub genes and immune cell infiltration. Moreover, the hub genes were examined for correlations with various immune factors, a total of 24 immunoinhibitors, 45 immunostimulators, and 41 chemokines are involved in the process (**Supplementary Table 2**), which were obtained from the TISIDB database [26].

Single-cell RNA sequencing (scRNA-seq) Data Analysis

scRNA-seq data from human coronary plaques, specifically obtained from stable angina pectoris (SAP) and acute coronary syndrome (ACS), were retrieved from the Gene Expression Omnibus public database (GEO) hosted by NCBI (https://www.ncbi.nlm.nih.gov/geo/). All steps involved in the processing of scRNA-seq data were conducted using R (version 4.0.5). A cell with fewer than 500 genes or with more than 10% mitochondrial genes was initially excluded from analysis. Furthermore, cells with more than 5000 genes were removed to mitigate potential doublets. The pre-processed data were then normalized and scaled using the NormalizeData function from the Seurat package. Subsequently, 2000 highly variable genes were identified using the Seurat FindVariableGenes function. Molecular cross-validation was employed to determine the optimal number of PCs to cluster the dataset effectively. The top genes specific to each population were

examined to annotate each cluster, and the FindAllMarkers function from the Seurat package was used to identify marker genes. To infer the origin and identify each cell type, the R package SingleR method was utilized, along with human transcriptomic datasets and corrected according to the cell signatures curated from the literature.

Mass Cytometry and Data Analysis

An Ethical Committee and Institutional Review Board of The Affiliated Hospital of Jiangsu University approved this study. Fresh peripheral blood samples were collected from the affiliated hospital of Jiangsu University, and all donors provided informed consent. Peripheral blood samples were obtained from both clinical AS patients and healthy individuals and collected in EDTA anticoagulant tubes (BD Biosciences). To process the samples, 2 mL of whole blood was mixed with 10 mL of ACK lysis buffer (eBioscience). The mixture was then centrifuged for 5 minutes to remove the supernatant, and the cells were washed three times with PBS before being stored on ice. For viability staining, the cells were washed and suspended with Live/Dead ^{194}Pt Cisplatin and incubated with Fc Receptors Blocker Mixture, followed by incubation with ^{191}Ir and ^{193}Ir DNA Intercalator at 4 °C overnight. Afterward, the cells were washed twice and stained with the antibody cocktail listed in **Supplementary Table 2**. Following staining, the cells were washed with double distilled water and pelleted before being loaded onto the Mass Cytometer platform (Polaris Starion X1), and the mass cytometry data were analyzed using FCS Express 7 De Novo software (Glendale, CA, United States).

Statistical Analysis

All analyses in this study were conducted using the R software, including the *t*-test and Mann-Whitney U-test. The choice between these tests depended on the distribution of the data. Statistical significance was defined as a p-value below 0.01.

Results

Identification of Hub Genes Associated with AS and Mitochondria-Related Metabolism

To identify AS-related genes, a total of 900 up-regulated and 601 down-regulated DEGs were selected from the combined GSE1000927 and GSE43292 datasets under the condition of p-value < 0.01 and a fold change >1.2, FDR <0.05 (Fig. 1A–C). A heatmap was generated to visualize the expression patterns of the top 15 differentially expressed genes (DEGs) between atherosclerotic lesions (AS, n = 101) and normal samples (NS, n = 67) (Fig. 1D). After filtering out abnormal samples and genes, a total of 168 samples and 5612 genes were used to construct a gene co-expression network using the WGCNA approach. The soft threshold power was assessed, and a value of 14 was chosen as it resulted in the successful construction of scale-free networks with an independence degree of up to 0.870 and an average connectivity of 0.626 (Fig. 2A,B). Using a merging threshold of 0.25 and a minimum module size of 30, a total of 9 distinct co-expression modules were identified through dynamic tree cutting (Fig. 2C). Correlation analysis revealed that the brown module exhibited the highest positive correlation with AS ($r = 0.67$, $p = 1.9 \times 10^{-23}$), while the grey60 module displayed the highest negative correlation with AS ($r = –0.60$, $p = 7.0 \times 10^{-18}$) (Fig. 2D,E). The grey module consisted of genes that did not belong to any specific module and did not exhibit significant reference relevance. Subsequent analysis focused on exploring the correlation between module membership (MM) and gene significance (GS). It was observed that the 350 genes within the brown module exhibited a strong positive correlation with both the module and AS phenotype ($r = 0.66$, $p = 2.4 \times 10^{-44}$) (Fig. 2F). Based on these findings, the 350 genes in the brown module were chosen for subsequent analysis. To identify hub genes related to metabolism and AS, we took the intersections of 2977 metabolism-related genes, 1501 DEGs, and the 350 genes from the brown module, leading to the identification of 10 hub genes (Fig. 3A). Violin plots showed that *NDUFS4* was expressed at lower levels in the AS group, while the other 9 genes showed significantly high expression in AS (Fig. 3C). And the expression of the hub genes in AS lesions compared to normal tissues were further confirmed via qRT-PCR (Fig. 3E), which showed a similar trend.

Hub Genes Enrichment in Biological Function and Pathways

The hub genes were analyzed through enrichment analysis to elucidate their potential biological roles. The GO analysis unveiled that *SLC11A1*, *SLC35C1*, *SLC37A2*, and *SLC16A4* hub genes were primarily associated with transmembrane transporter activity, antiporter activity, phosphate antiporter activity, and similar functions. Additionally, *CHKA* was found to be primarily involved in cholinesterase activity (Fig. 3B,D). Furthermore, GSEA analysis of gene sets demonstrated significant enrichment of the 10 hub genes in relation to inflammation and immune function, such as the NOD-like receptor signaling pathway, renin-angiotensin system, chemokine signaling pathway, primary immunodeficiency, and hematopoiesis (Fig. 4A). Single-genes GSEA results also showed similar results (Fig. 4B–K). Notably, the low expression of *NDUFS4* was significantly correlated with immune-related signals, while the high expression of the remaining 9 hub genes showed a similar association with these pathways.

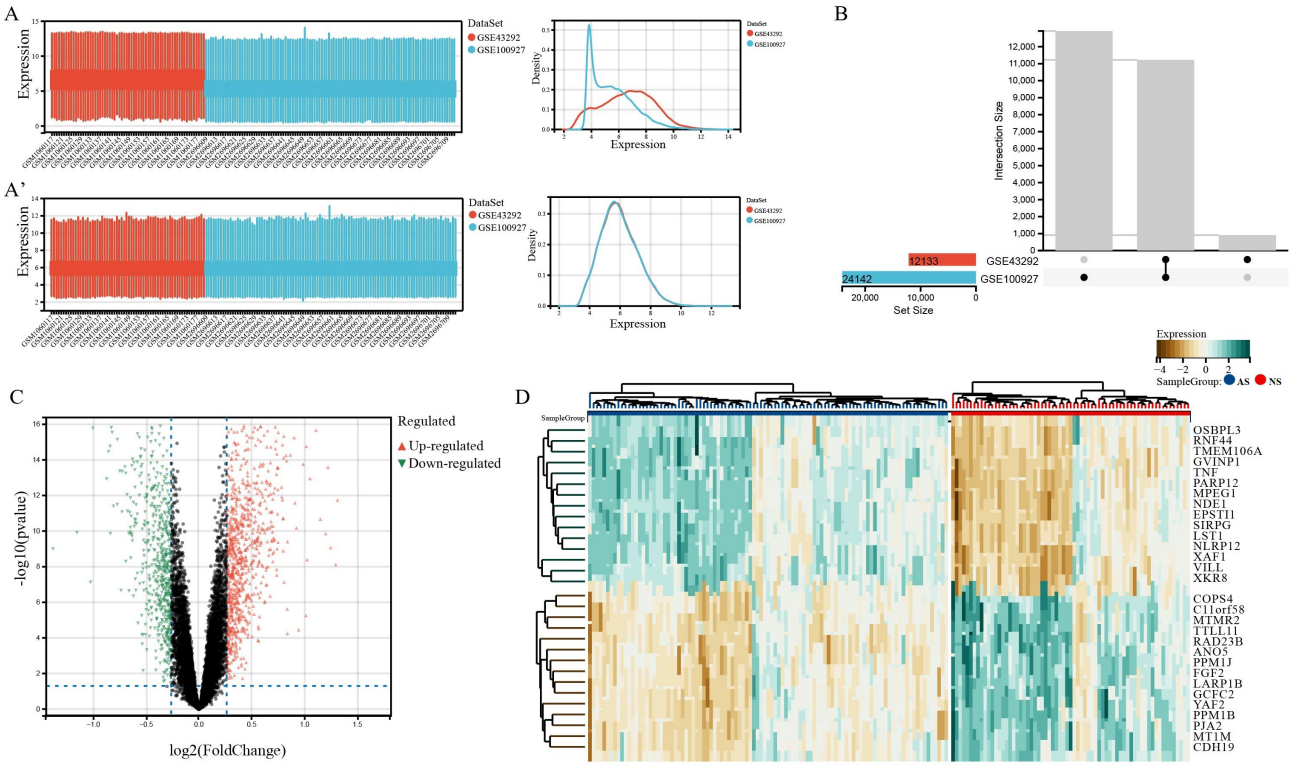

Fig. 1. Differentially expressed genes between the AS and NS group. (A) Merging and normalization of the two datasets. (B) Intersection between the two datasets after merging. (C) Differential gene volcano plot, where red represents genes highly expressed in the AS group compared to the NS group, green represents genes with low expression, and black represents genes with no significant difference. (D) The heatmap of 15 most highly expreesed genes expression.

Diagnostic Assessments of Hub Genes via Machine Learning

To assess the diagnostic value and the association of these hub genes with the risk of AS, random forest and LASSO regression machine learning algorithms were used. First, logistic multivariate regression analysis was performed (Fig. 5A). The random forest plots, generated after conducting COX proportional hazards regression analysis, displayed the risk ratios associated with the 10 hub genes. In the plot, the position of each gene is indicative of its association with the risk of AS. Specifically, *ARSB* was positioned to the left of the invalid line, suggesting it as a protective factor for AS. Comparatively, *TNF* was situated to the right of the vertical dash line, indicating it as a risk factor for AS (Fig. 5A). The LASSO regression algorithm identified seven potential hub genes as well (Fig. 5A). Notably, *TNF* showed a significant and positive correlation, while *ARSB* showed a significant but negative association. Then, *ARSB* and *TNF* were selected to construct a diagnostic model using stepwise regression analysis. The corresponding AUC was calculated (Fig. 5B), and the ROC curve and high AUC (0.93) suggested that based on this model, some guiding principles can be derived to diagnose AS in clinical applications.

Correlation between Hub Genes, Immune Microenvironment and Immunologic Factors

Based on the functional enrichment results suggesting the enrichment of hub genes associated with AS pathogenesis in immune regulation pathways, we further investigated the immunomodulation properties in AS through an analysis of immune cell infiltration. The CIBERSORT algorithm was utilized to estimate the proportions of 22 immune cell types in the 168 samples, and the resulting proportions for each sample are presented in the histogram (Fig. 6A). The boxplot in Fig. 6B demonstrates the differences in immune cell infiltration between AS and NS samples, showing that AS patients had a higher level of B memory cells, plasma cells, $CD8^+$ T cells and M0 macrophages ($p < 0.001$), whereas the levels of resting memory $CD4^+$ T cells, monocytes, resting mast cells and eosinophils were significantly decreased ($p < 0.001$). Fig. 6C further illustrates the correlations between immune cells, revealing that resting memory $CD4^+$ T cells are negatively associated with M0 macrophages (r = –0.64) and $CD8^+$ T cells (r = –0.62), while monocytes show a positive relationship with activated dendritic cells (r = 0.59) (Fig. 6C). Subsequently, we analyzed the relationships between the hub genes and immune infiltration cells, as well as immune factors such as immune inhibitors, immune stimulators, and immune chemokines. Notably, *SLC37A2* exhibited a sig-

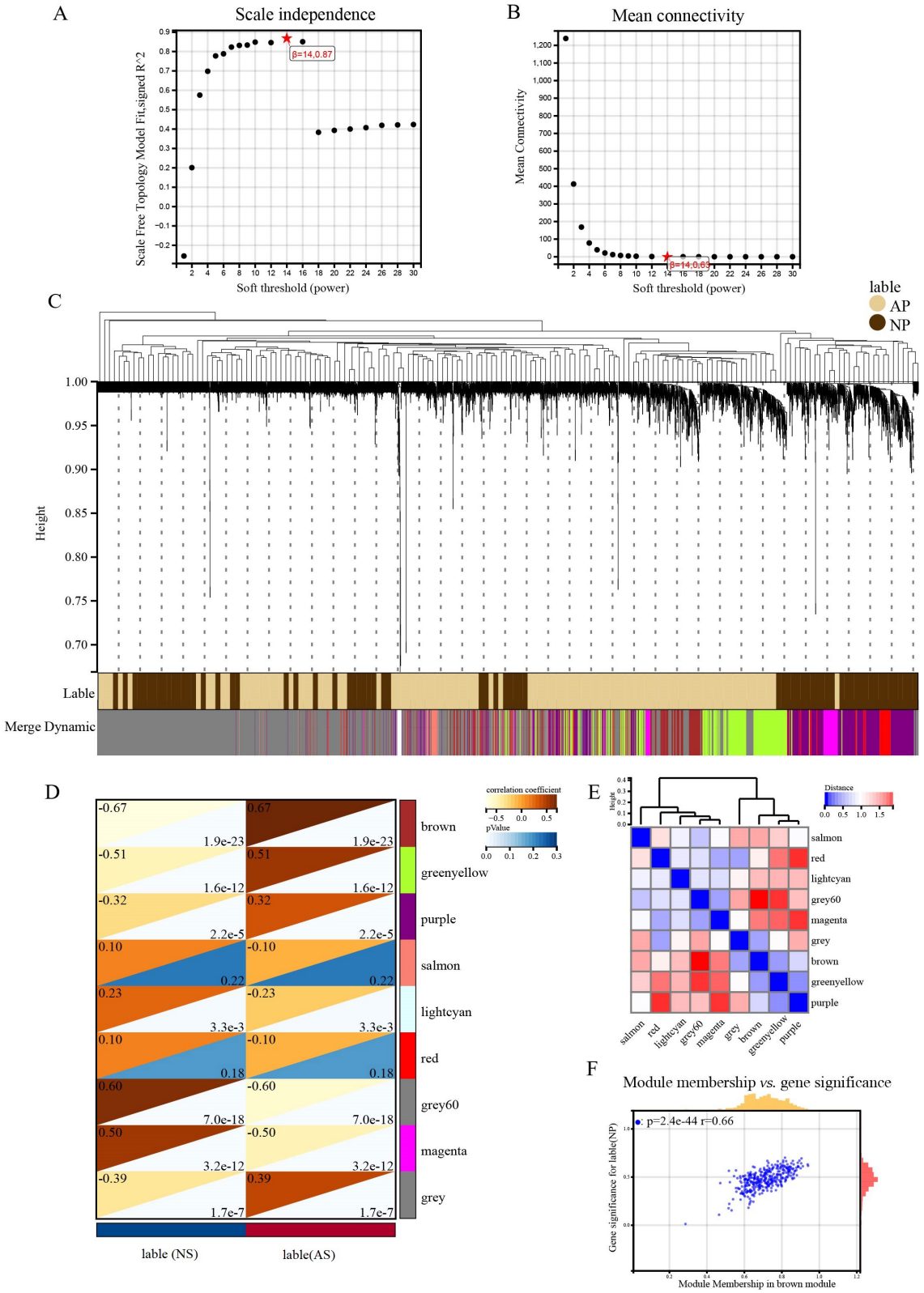

Fig. 2. WGCNA analysis indicates AS-related hub genes. The scale-free topological model fit indices and mean connectivity values were calculated at various soft threshold powers and shown in (A) and (B), respectively. (C) Cluster dendrogram of genes. (D) Correlation between various modules and clinical traits, with red indicating a positive correlation and blue indicating a negative correlation. (E) Correlations between different module memberships. (F) Correlation of module membership and gene significance in the turquoise module.

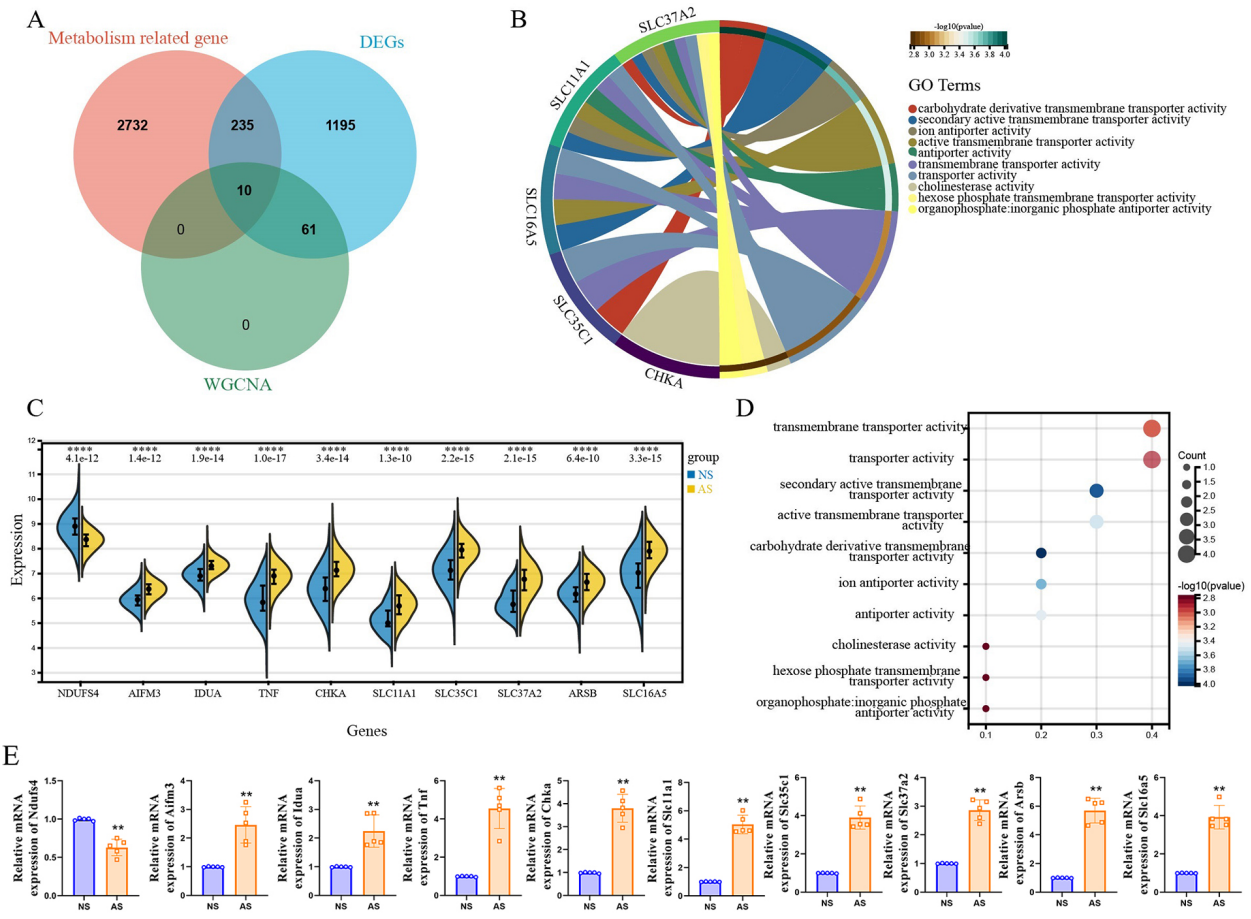

Fig. 3. Hub genes and Gene Ontology (GO) analysis. (A) Ten hub genes were obtained by taking the intersections of the metabolism-related genes, DEGs and hub genes of WGCNA analysis. (C) The expression of ten hub genes in the AS and NS group (****p-value < 0.0001 *vs.* NS group). (B,D) Biological processes in which the hub genes could be involved. (E) qRT-PCR confirmed the hub genes expression in AS lesions and normal tissues, (**p-value < 0.01 *vs.* NS group), the *in vitro* tests were repeated at least three times independently.

nificant negative association with $CD4^+$ Tem cells and a positive correlation with M0 macrophages (Fig. 7A). Moreover, based on the correlation heatmaps, the hub genes displayed significant correlations with immune inhibitors, immune stimulators, and chemokines (Fig. 7B–D), indicating their potential importance in regulating the immune microenvironment.

Heterogeneity of Immune Cells in the Atherosclerotic Plaque Microenvironment

Identifying the immune microenvironment and metabolic characteristics of atherosclerotic plaques at the single-cell level will provide further insights, we analyzed single-cell sequencing data from patients with atherosclerosis in both the acute and stable phases. First, data pre-processing was performed to obtain clean raw data by eliminating doublets and mitochondrial contaminations (Fig. 8A). Then, we utilized an unsupervised cluster detection algorithm to identify cell clusters with similar gene expression among $CD45^+$ cells. These cell clusters were primarily differentiated and named based on hematopoietic lineage genes, such as ITGAM, CD19 and CD3. The UMAP plot displayed the distribution of the cell subpopulations (Fig. 8B). The next step was to analyze differential gene expression, and each subpopulation to validate the identification of the respective cell subpopulations (Fig. 8C,D). The violin plot in Fig. 8E illustrates the expression of metabolic-related hub genes across various immune cell types. We observed that *TNF* was predominantly expressed in T cells and monocytes/macrophages, while *SLC11A1* and *NDUFS4* were mainly expressed in monocytes/macrophages. By comparing the distribution of immune cells in atherosclerotic plaques between patients in the acute and stable phases (Fig. 8F,G), we discovered a significant increase in immune cell infiltration in the acute phase plaques, with evident heterogeneity. Moreover, *SLC11A1* and *NDUFS4* expression was mainly concentrated in monocytes and T cells in acute phase plaques, while *TNF* was mainly expressed in T cells in stable phase plaques.

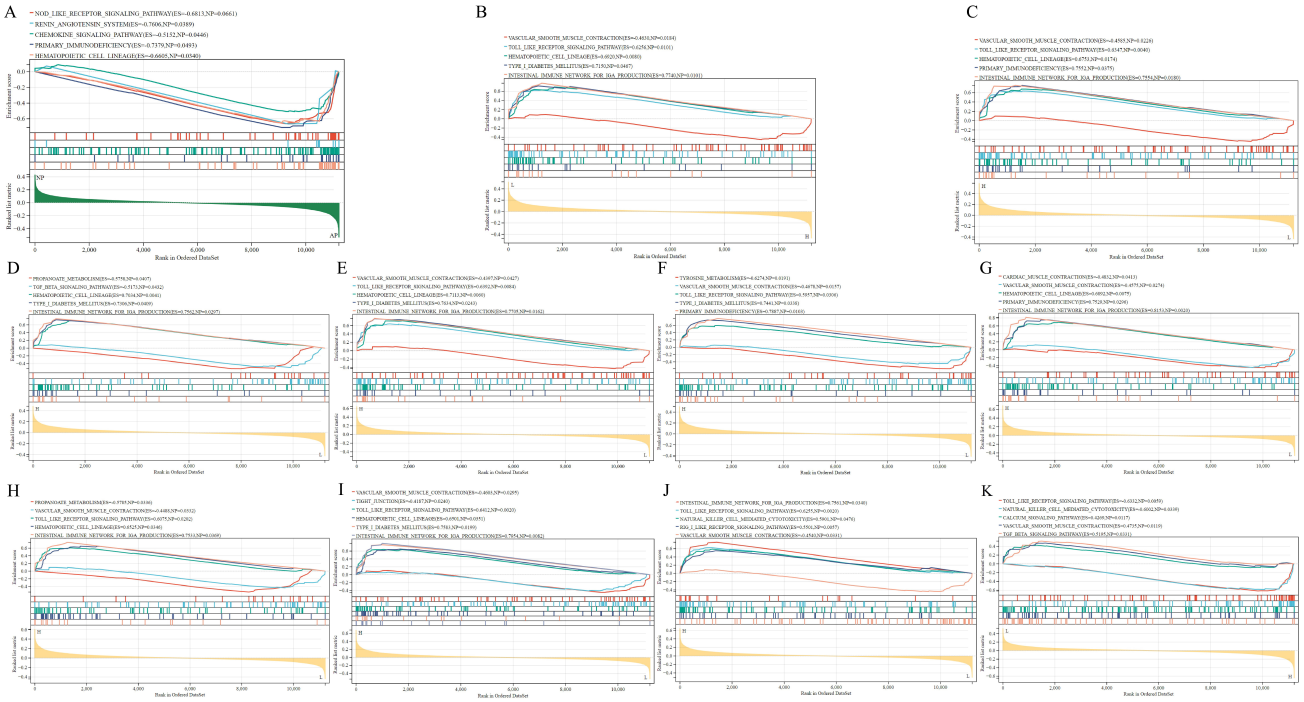

Fig. 4. GSEA reveals the enriched pathways of the hub genes. (A) The hub genes are distinctly enriched in several common pathways. (B) *NDUFS4*. (C) *AIFM3*. (D) *IDUA*. (E) *TNF*. (F) *CHKA*. (G) *SLC11A1*. (H) *SLC35C1*. (I) *SLC37A2*. (J) *ARSB*. (K) *SLC16A5*.

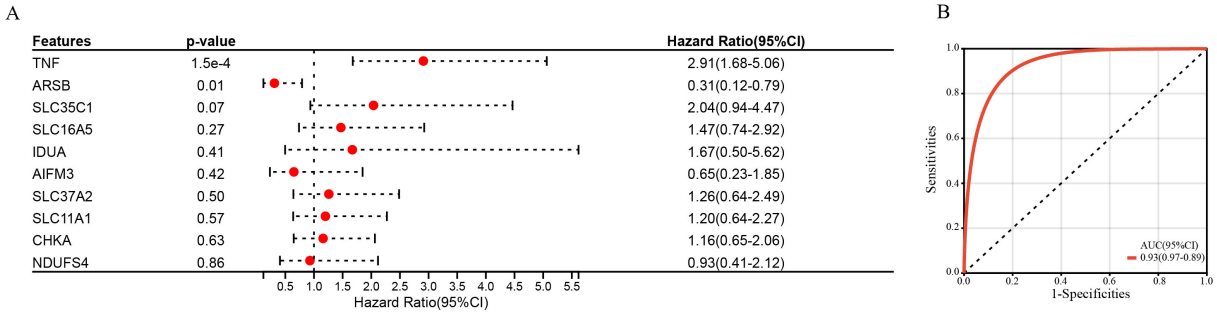

Fig. 5. Random forest and ROC curve analysis. (A) Variable importance plot of the random forest model. (B) The ROC curve of *TNF* and *ARSB* model.

Mass Cytometry (CyTOF) Exhibits the Peripheral Immune Cell Repertoire in Atherosclerosis Patients

Vascular inflammation is widely acknowledged as a significant factor contributing to the erosion and rupture of AS plaques. However, the precise immune microenvironment and immune responses driving plaque progression in atherosclerosis remain unclear. To address this knowledge gap, we comprehensively characterized the peripheral blood immune cell profile in both healthy individuals and atherosclerotic patients using mass cytometry analysis, comprising three individuals in each group. Each sample consisted of approximately 6×10^6 $CD45^+$ cells. Fig. 9A shows the gating strategy for cell subpopulations. Based on the expression of classical immunophenotype markers, we annotated five main peripheral blood immune cell types, namely granulocytes, monocytes, T cells, B cells and NK cells. Furthermore, monocytes were further subclassified into classical monocytes, intermediate monocytes, and nonclassical monocytes based on the expression of CD14 and CD16. Similarly, T cells were subdivided into $\alpha\beta$T and $\gamma\delta$T cells, with further classification based on relevant classical markers. According to the expression of CD27 and IgD, B cells were classified into naive, switched memory, and nonswitched memory B cells. Subsequently, tSNE clustering analysis of normal and AS samples revealed distinct distributions of peripheral blood immune cells in AS patients compared to healthy controls (Fig. 9B). The changes in the proportions of each cell subpopulation were visualized using a sunburst chart (Fig. 9C). Statistical analyses demonstrated that AS patients exhibited higher numbers of $CD4^+$ T cells and $CD8^+$ T cells in their peripheral blood compared to healthy individuals. In contrast, the number of monocytes, particularly classical monocytes ($CD14^+CD16^-$), in AS patients were reduced (Fig. 9D).

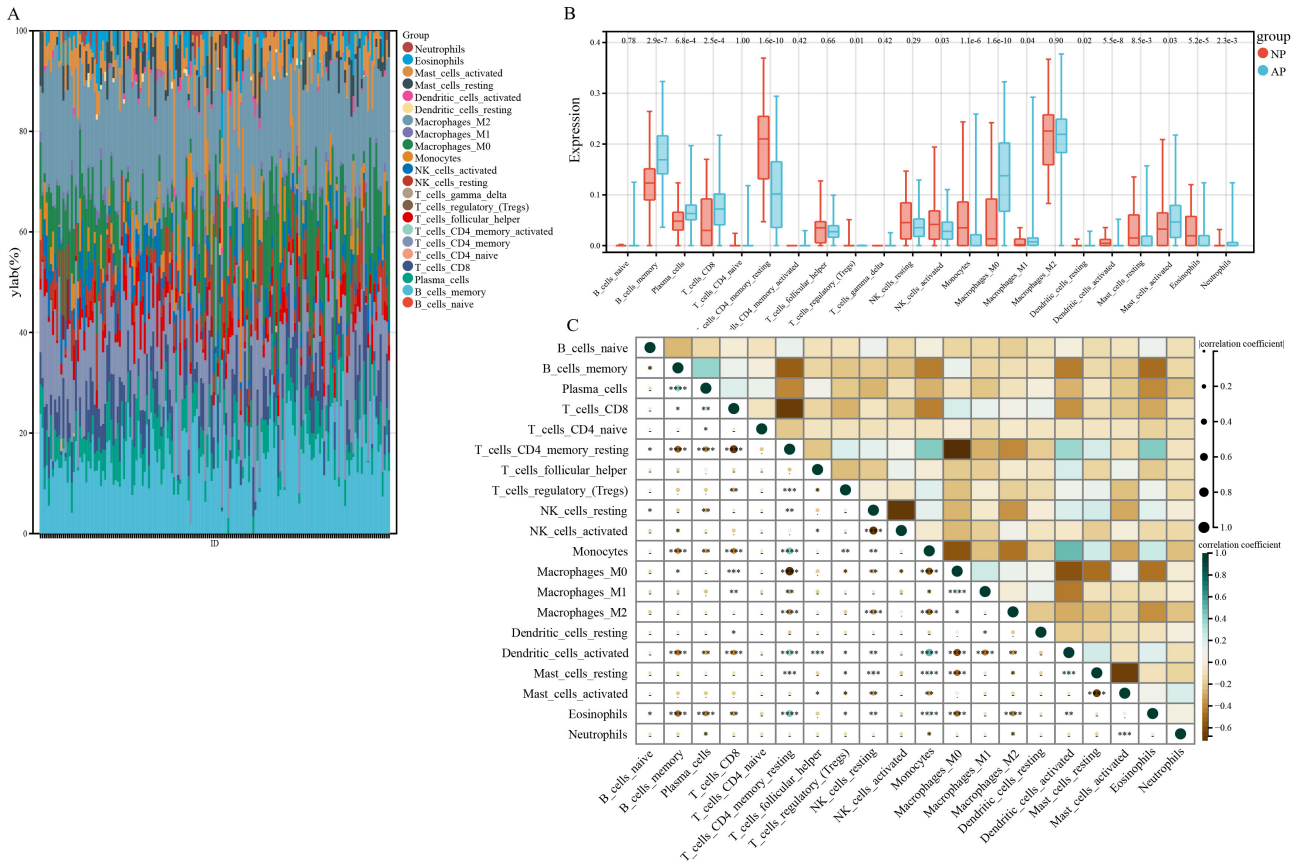

Fig. 6. Immune infiltration in the AS and NS group. (A) The relative percentage of 22 immune cells in each sample. (B) Differences in immune infiltration between the AS and NS group. (C) The correlations between different immune cells (Lower *p* values represent more significant correlations, **p*-value < 0.05, ***p*-value < 0.01, ****p*-value < 0.001, *****p*-value < 0.0001).

Discussion

AS and its associated complications, such as myocardial infarction and unstable angina, are the main causes of mortality in patients with atherosclerotic cardiovascular disease (ASCVD). The pathogenesis of AS has been extensively studied, with an increasing focus on its association with prognosis, metabolism and the immune microenvironment. AS is recognized as a chronic inflammatory disease, and mechanisms involving inflammation and lipid metabolism disorder contribute to its accelerated progression [27]. Traditionally, AS was believed to result from passive lipid deposition on vascular walls. However, recent studies have revealed the complexity of AS etiology, highlighting the crucial roles of immune regulation and metabolic changes, as well as their interactions, in AS pathogenesis [28]. In this study, we conducted differential analysis, WGCNA and functional enrichment analysis using two gene expression datasets (GSE100927 and GSE43292) to identify key genes associated with mitochondrial metabolism and AS pathogenesis. Using random forest and LASSO regression learning algorithms, we identified hub genes with potential diagnostic value and examined their correlation with immune infiltration levels and various immune factors, placing particular emphasis on their expression patterns. To further expand our understanding, we analyzed single-cell sequencing data (GSE184073) to explore the immune microenvironment profiles of AS plaques in both the acute and stable phases, and examined the expression of the identified hub genes in specific immune cell subsets. Additionally, we validated the immune cell composition in the peripheral blood of AS patients using mass spectrometry-flow cytometry, enabling multi-dimensional analysis of immune cell composition. Through these comprehensive evaluations, we aimed to gain deeper insights into the regulation of the AS plaque microenvironment by immune and metabolic factors, evaluate the significance of immunity and metabolism in AS, and identify potential therapeutic targets for AS treatment.

In this study, we identified 10 genes closely associated with mitochondria-related metabolism and AS. Machine learning was implemented to screen for the hub genes with diagnostic and prognostic significance in AS, based on which the *TNF* and *ARSB* were identified (Fig. 5). GO functional enrichment results indicated that the functions of hub genes such as *SLC11A1*, *SLC35C1*, *SLC37A2*, and *SLC16A4* are mainly associated with transmembrane transporter activity, antiporter activity and phosphate an-

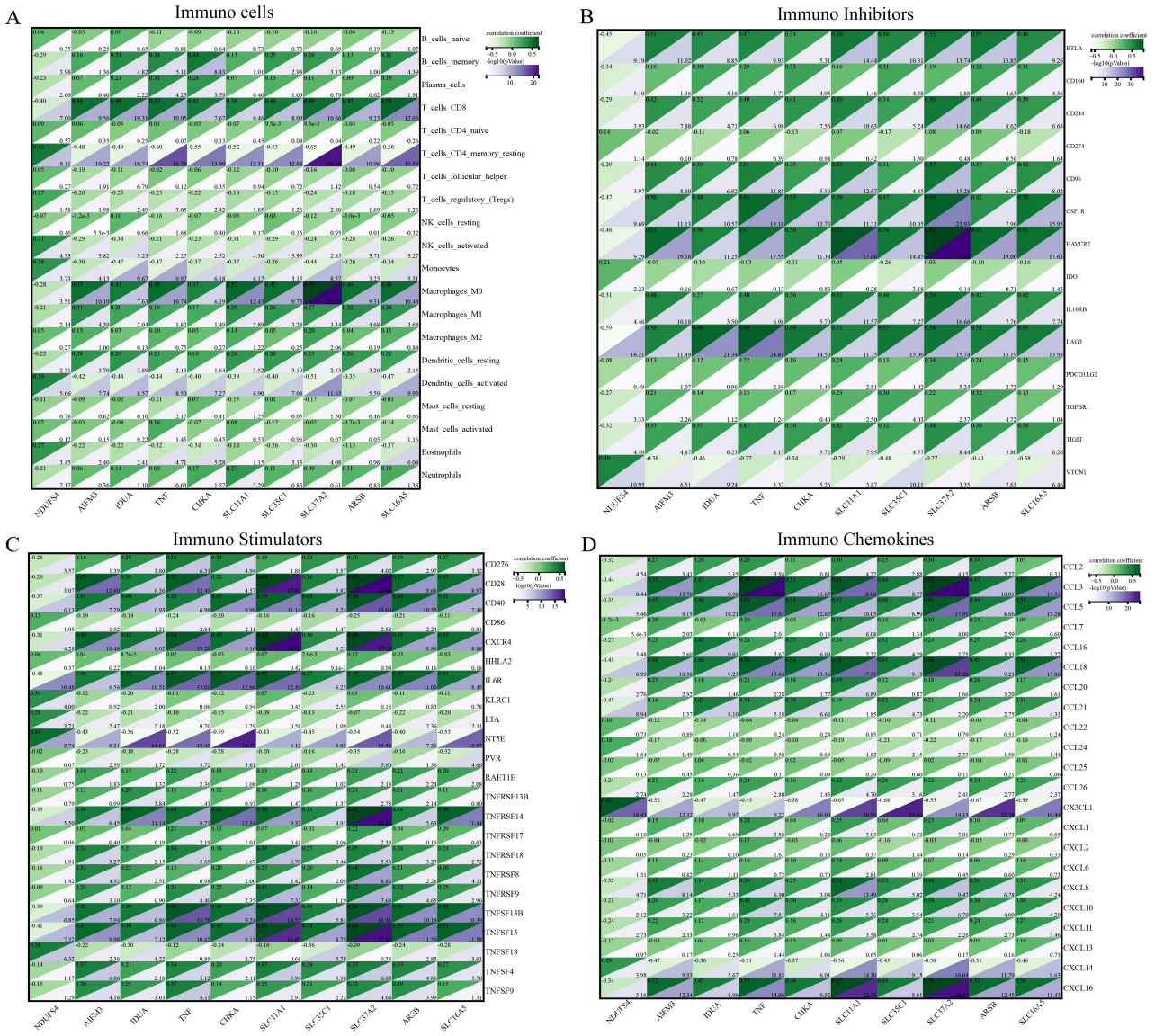

Fig. 7. Correlation of hub genes with immune cells and different immune factors. (A) Immuno cells. (B) Immuno inhibitors. (C) Immuno stimulators. (D) Immuno chemokines.

tiporter activity, while *CHKA* was primarily involved in cholinesterase activity (Fig. 3B,D). Transmembrane transporter activity has been reported to be associated with oxidative stress response biological process [29], with oxidative stress induced by excessive levels of reactive oxygen species shown to be an important mechanism associated with AS occurrence [30]. *SLC11A1*, *SLC35C1*, *SLC37A2*, and *SLC16A4* belong to the solute carrier family, and previous studies have highlighted the diverse roles of *SLC11A1* in macrophage activation and immune responses [31]. However, the specific involvement of *SLC11A1* in AS has not been extensively investigated, as most studies have focused on its relevance to tumor-related diseases [32], inflammatory bowel disease [33] and bacterial infections [34,35]. *SLC35C*, also known as GDP-fucose transporter 1, *CDG2C* or *FUCT1*, acts as a negative regulator of the canonical Wnt signaling pathway. Studies have demonstrated that *SLC35C1* deletion can activate the Wnt pathway, promoting colon cancer progression [36], and *SLC35C1* mutation can cause fucosylation disorder, leading to genetic diseases [37]. Interestingly, fucosylation has been implicated in early AS, where it is associated with reduced cell migration and the accumulation of cholesterol-rich foam cells in the tunica intima of blood vessels [38]. We speculate that *SLC35C1* may be an active therapeutic target for the early prevention and control of AS.

SLC37A2 is a phosphate-linked glucose-6-phosphate transporter located in the endoplasmic reticulum, predominantly expressed in macrophages and neutrophils, and has been shown to play a significant role in inflammatory activation and glycolytic reprogramming in macrophages [39]. Studies have reported that hematopoietic cell-specific knockout of *SLC37A2* can accelerate atherosclerosis in LDL receptor-deficient mice [40]. However, further in-

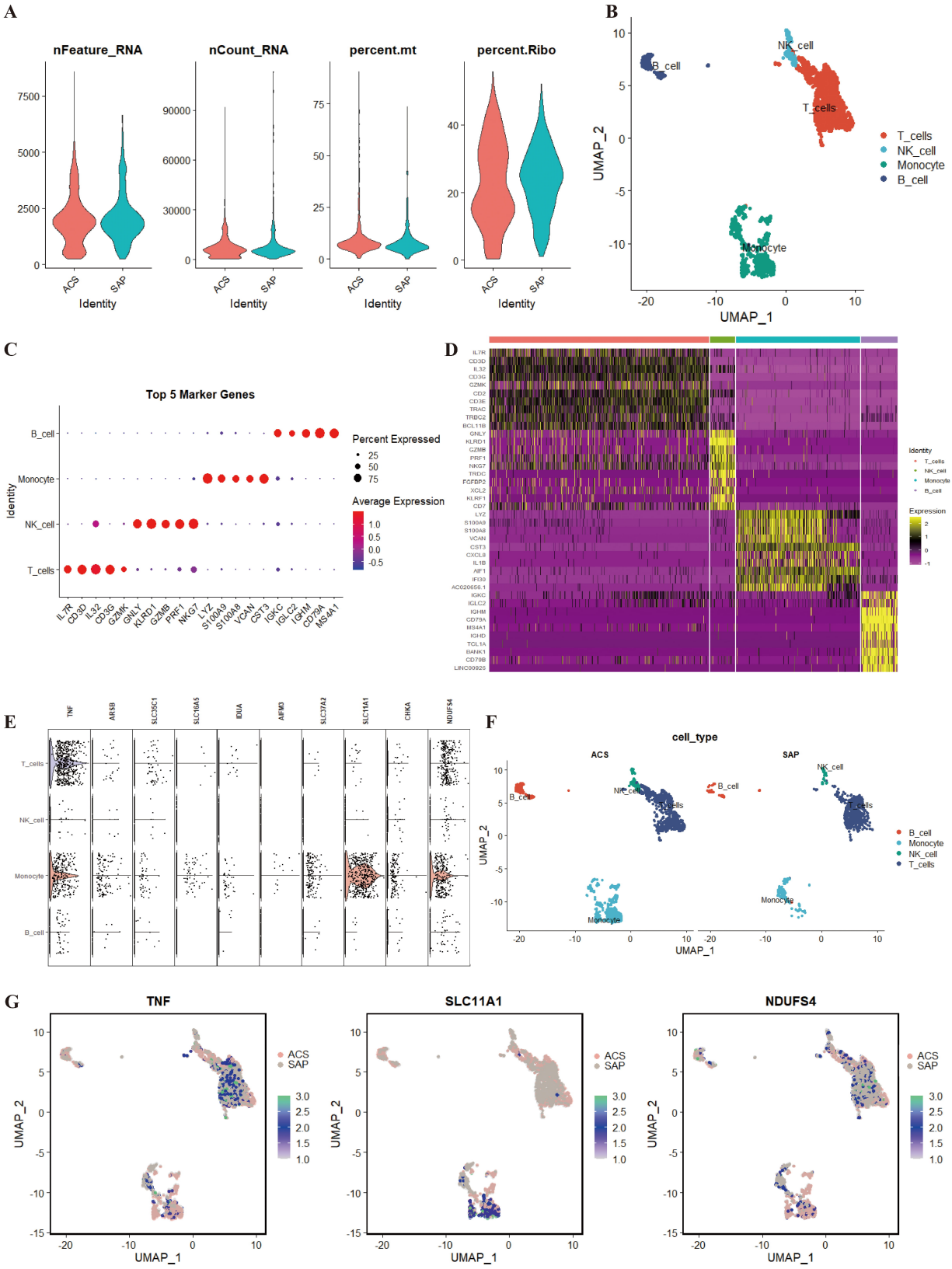

Fig. 8. scRNA-seq analysis of ACS and SAP sample. (A) Quality control for scRNA-seq data. (B) spectral t-SNE plot of CD45^{+} immune cells composition after unsupervised clustering. (C) Dot plot of known marker genes identifying cell type. (D) Heatmap of top 5 marker genes for each cluster. (E) The expression of hub genes in each cell type. (F) The differences in the composition of immune cells in ACS and SAP samples. (G) The *TNF*, *SLC11A1* and *NDUFS4* gene expression distributions of cell type in ACS and SAP.

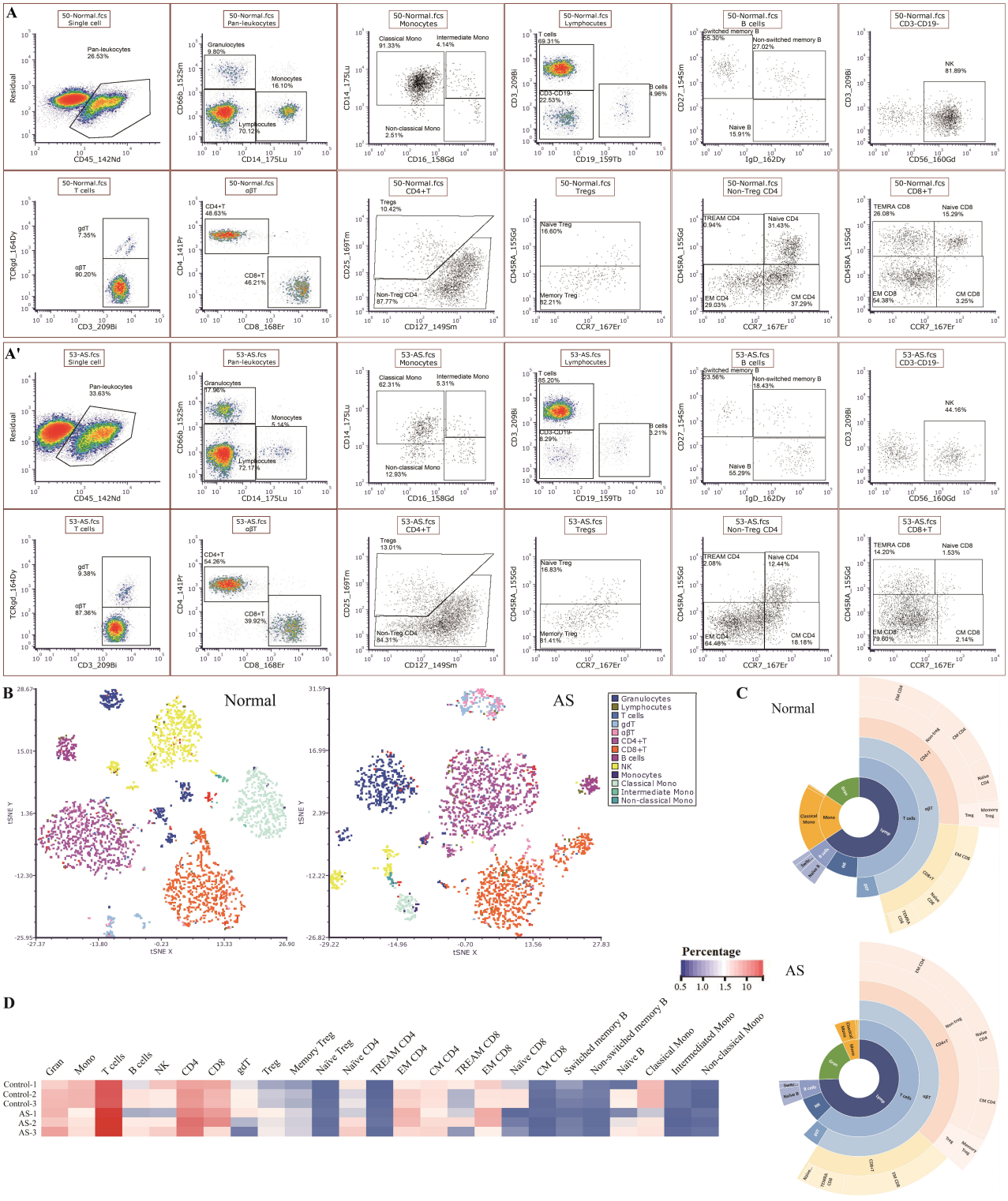

Fig. 9. The peripheral blood immune cell profile of healthy people and AS patients via mass cytometry. (A) Gating strategies for immune cell subsets. (B) Spectral t-SNE plot of immune cells composition after unsupervised clustering. (C) Sunrise chart demonstrating the percentages of each cell subpopulation. (D) Heatmap showing the changes in cell subpopulations' percentage.

vestigations are required to elucidate the precise relationship between *SLC37A2* and AS pathogenesis. A *SLC16A4*, also known as *MCT4*, is a monocarboxylate transporter with a high affinity for lactic acid transport [41]. It primarily functions to maintain intracellular pH homeostasis and is often found to be overexpressed in various tumor types. Lactic acid is mainly produced through glycolysis in tumors and was only recently discovered to be the main fuel and signal inducer in cancer cells [42]. It plays diverse roles, including serving as an energy source, a precursor

for gluconeogenesis, and a signaling molecule, and it is involved in metabolic interactions between energy-producing and energy-consuming cells. Recent research has expanded the understanding of lactic acid beyond tumors and cardiovascular diseases, revealing its significance in the immune microenvironment. Metabolic reprogramming of cardiomyocytes, a hallmark of heart failure, involves altered mitochondrial keto acid oxidation and increased lactic acid export. This metabolic axis, involving the mitochondrial pyruvate carrier and *SLC16A4*, plays a crucial role in cardiomyocyte metabolism [43]. Lactic acid-associated lactylation has been found to be widespread in the human proteome and is involved in the regulation of various inflammatory disorders. Considering the cellular distribution and metabolic characteristics within atherosclerotic plaques, the glycolysis-lactic acid-lactylation axis may represent a novel avenue for future AS-targeted intervention. However, further investigations are needed to elucidate the specific role of *SLC16A4* in AS pathogenesis. Lipid droplets are dynamic lipid-rich organelles that serve as major sites for cholesterol storage in macrophage foam cells and are potential targets for AS treatment [44,45], and can be considered a central hub of cell metabolism and the immune system [46].

CHKA, a member of the choline kinase family, plays a crucial role in catalyzing the phosphorylation of free choline to phosphocholine, which is further converted to cytidine diphosphate (CDP)-choline by cholinephosphate cytidylyltransferases (CCT) and subsequently to phosphatidylcholine (PC) by cholinephosphotransferase-1 (*CHPT1*). Alternative splicing of the *CHKA* gene produces *CHK*α*2*, which can bind to lipid droplets and is crucial for lipid droplet lipolysis. This process is regulated by AMP-activated protein kinase (AMPK) [47]. Overexpression of *CHKA* has been observed in various cancers and is associated with tumor prognosis. Consequently, *CHKA* has emerged as a target for cancer treatment and its regulatory role in AS warrants further investigation. *TNF*, secreted primarily by macrophages, is a crucial inflammatory factor implicated in AS pathogenesis [48–50]. Comparatively, *ARSB*, a member of the sulfatase family, can target lysozymes, but its role in AS pathogenesis has not been reported, with only a research study by Biros *et al*. [51] reporting on the potential association of *ARSB* upregulation with cerebral embolism. Interestingly, some progress has been reached in AS clinical treatment using L-ascorbic acid as an antioxidant [52,53]. In addition, L-ascorbic acid can also function as an ARSB inhibitor, suggesting that it may be a new therapeutic target for AS.

GSEA results revealed that the 10 hub genes related to mitochondria metabolism, significantly enriched in pathways associated with inflammation and immunity, such as NOD-like receptor signaling, renin-angiotensin system, chemokine signaling pathway, primary immunodeficiency, and hematopoietic pathways. This finding highlights the intricate interplay between metabolism, inflammation, and the immune system in the development of AS. Accumulating evidence suggests that AS-associated factors induce significant metabolic reprogramming in immune cells within the plaque microenvironment, ultimately influencing AS plaque formation [54]. *NLRP3* inflammasome, a member of the NOD-like receptor family, plays a vital role in AS. This inflammasome links lipid metabolism with sterile inflammation [55]. The mitochondrial electron transport chain is crucial for *NLRP3* inflammasome activation [56], and fatty acids and cholesterol also play key roles in regulating *NLRP3* inflammasome [57]. In addition, a study reported that *NLRP3* inflammasome activation in macrophages is negatively correlated with glycolysis, and inhibiting glycolysis may activate the *NLRP3* inflammasome [58]. AS is strongly linked to the renin-angiotensin system (RAS), which is involved in controlling cardiovascular function and affecting AS progression [59]. Various cell types within AS plaques express components of RAS, including angiotensinogen, angiotensin I, angiotensin-converting enzyme, and angiotensin II type 1 receptor. Changes in the distribution and expression levels of RAS components occur during AS progression [60], and RAS activation can affect the expression of inflammatory factors and regulate inflammatory responses through various signaling pathways [61].

The interactions between metabolism and inflammation/immunity in AS are yet to be validated in subsequent research. The findings from Fig. 6B indicate that atherosclerotic plaques have higher levels of B memory cells, plasma cells, $CD8^+$ T cells, and M0 macrophages, while resting memory $CD4^+$ T cells, monocytes, resting foam cells and acidic granulocytes are significantly reduced. The immune infiltration analysis results of CIBERSORT demonstrated the immune regulation characteristics in AS. Furthermore, Fernandez *et al*. [62] discovered that AS plaques exhibit a unique immune microenvironment, in which macrophages act as drivers for plaque instability and other immune cells, such as T cells and B cells, also play important regulatory roles. Our analysis of single-cell sequencing data from active and stable AS plaques revealed that T cells are the most abundant immune cells in the plaques and exhibit substantial heterogeneity, with distinct populations observed in active and stable plaques (Fig. 8B,F). These findings suggest that immuno cells may have significant involvement in AS plaque formation and rupture as reported before. Additionally, B cells have been shown to activate cellular immunity in AS, and their direct regulation of T-cell activity through antigen presentation, co-stimulation and cytokine production has been highlighted in previous studies [63].

We also assessed the relationship between the immune microenvironment profile in AS plaques and metabolism. On the basis of the aforementioned analysis, we reexamined the correlation between hub genes and immune infiltration cells. The heat map illustrates that these hub genes strongly correlate with different immune factors. *TIM-3*, also known

as *HAVCR2*, is a type 1 transmembrane protein that regulates innate and adaptive immune responses. It affects several immune cell functions [64]. Tim3 can also inhibit Platelet-Derived Growth Factor-BB (PDGF-BB)-induced AS responses in human arterial smooth muscle cells [65], promote angiogenesis, and decrease tight junctions between vascular endothelial cells [66]. Our analysis results indicated that *HAVCR2* expression may be closely associated with *SLC11A1* and *SLC37A2*. A recent study showed that *LAG3* can regulate T-cell activation and plaque infiltration in AS mice [67]. Increasing attention is focused on the role of immune checkpoints in cardiovascular diseases. Although Immune Checkpoint Inhibitor (ICI) therapy has provided a successful treatment option for cancer patients and may improve patients' prognosis, the interactions of ICI therapy with the cardiovascular system might result in consequential risks [68]. Therefore, there is a need for a more in-depth understanding of the mechanism behind cardiovascular disease regulation by immune checkpoints. *CXCR4* is a critical marker for recognizing B1 cells that produce IgM to malondialdehyde-LDL in the human body. MDA-LDL production is enhanced when B1a cells express *CXCR4* and migrate toward the bone marrow. In addition, *CXCR4* expression on human $CD20^{+}CD27^{+}CD43^{+}$ B1 cells is negatively correlated with coronary artery plaque burden and necrosis [69]. It has been shown that conditional knockout of *CXCR4* in the B cells of mice can lead to increased severity of AS [70]. The $CCL2^{-}CCR2$ axis tightly regulates the mobilization of inflammatory monocytes, and defects in CCR2 expression result in reduced AS lesions [71]. During inflammation, activated platelets deposit *CCL5* on arterial endothelium, contributing to the recruitment of leukocytes and plaque formation [72]. *CX3CL1* is a structurally and functionally unique chemokine that can promote the adhesion of leukocytes to the vascular walls, has cytotoxic effects on endothelial cells, and is a major pathogenic factor in AS occurrence and plaque instability [73]. In addition, *CCL5* and *CCL18* have been identified as independent risk factors for short-term mortality in acute coronary syndrome patients [74] and potential diagnostic and prognostic parameters for stable coronary artery disease patients [75].

The role of vasculitis in driving plaque erosion and rupture in atherosclerosis (AS) is widely recognized. However, the immune microenvironment within AS lesions and the immune responses contributing to plaque progression remain poorly understood. Herein, we utilized mass spectrometry-flow cytometry to further analyze the peripheral blood immune cell profile of healthy individuals and AS patients. The monocyte is the most abundant immune cell in the peripheral blood, and plays a key role in bridging innate and adaptive immunity as well as regulating inflammation [76]. There are phenotypic and functional differences in peripheral blood monocyte subsets based on the expression of CD14 and CD16, indicating the different proinflammatory profiles and migration potential associated with AS occurrence [77]. In addition to monocytes, T cells from the peripheral blood are recruited to plaques and actively interact with antigen-presenting cells. This interaction leads to T cell activation, differentiation, expansion of antigen-specific TCR repertoire, and production of inflammatory cytokines, thereby contributing to the progression of AS [78]. Clinical evidence suggests that alterations in specific T-cell subsets, such as Th1, Th17, Treg, and $CD8^{+}$ T cells in peripheral blood, are closely linked to AS risk [79,80], suggesting the feasibility of using peripheral blood immune cell distribution as a biomarker for predicting AS risk. Single-cell sequencing analysis further corroborates that during the acute formation of atherosclerotic plaques, monocytes/macrophages with elevated expression of *SLC11A1* play a pivotal role, hinting at the potential of *SLC11A1* as a crucial regulatory target for macrophage activation and the immune response [31]. *NDUFS4* has been reported to negatively modulate pro-inflammatory macrophage activation and the shift to glycolytic metabolism [81], and it can mitigate inflammation and augment bone resorption by altering macrophage-osteoclast polarization [82]. Conversely, mitochondrial dysfunction in $Ndufs4^{-/-}$ mice led to reduced cholesterol synthesis, even though it resulted in decreased motor function in these mice [83]. Collectively, the insights derived from single-cell sequencing highlight the intricate immune microenvironment of atherosclerotic plaques and offer a perspective to understand the pathogenesis of AS and significant immunoregulatory targets from a mitochondrial metabolism standpoint.

While previous studies have investigated metabolism or immune regulation hub genes in AS [84,85], very few have utilized advanced bioinformatics techniques to explore their shared molecular mechanisms. Our study identifies common DEGs and hub genes, elucidates their functions, and sheds light on the mechanisms underlying metabolism-immunity interactions in AS. However, our study also has limitations, and further experimental validation of the hub genes and their functions, as well as their potential as therapeutic targets, is warranted, which will be the focus of our future work. The identified hub genes linking AS, mitochondria-related metabolism, and immune regulation hold potential as diagnostic markers and therapeutic targets for future AS research. The interplay between metabolism and immunity sheds light on AS pathogenesis, suggesting new avenues for treatment. The identified hub genes linking AS, mitochondria-related metabolism, and immune regulation hold potential as diagnostic markers and therapeutic targets for future AS research. The interplay between metabolism and immunity sheds light on AS pathogenesis, suggesting new avenues for treatment.

Conclusions

In conclusion, our study identified 10 hub genes that serve as crucial links connecting AS, mitochondria-related

metabolism and immune regulation. We elucidated the biological processes and pathways associated with these genes and conducted validation analyses using monocytes from atherosclerotic plaques in the acute and stable phases. Additionally, we investigated the changes in the peripheral blood immune cell profile in AS. These findings contribute to a better understanding of the interplay between AS pathogenesis, metabolism and immunity. Furthermore, we developed a diagnostic model based on logistic regression analysis, demonstrating its potential for predicting the risk and progression of AS and holding promise for clinical applications. Overall, our study provides novel insights into the intricate relationships between metabolism and immunity in AS, proposing potential targets for therapeutic interventions in clinical settings.

Availability of Data and Materials

A description of the original contributions to the study is provided in the article and Supplementary Materials. For further information, can directly contact the corresponding authors.

Author Contributions

FL developed a major research plan. FL and TL analyzed data, drew charts. FL and XL write manuscripts. XL finish the interpretation of data for the research. TL and DQ collect data and finish experiments. All authors contributed to the article and approved the submitted version. All authors contributed to editorial changes in the manuscript. All authors read and approved the final manuscript. All authors have participated sufficiently in the work to take public responsibility for appropriate portions of the content and agreed to be accountable for all aspects of the work in ensuring that questions related to its accuracy or integrity.

Ethics Approval and Consent to Participate

Not applicable.

Acknowledgment

Not applicable.

Funding

This work was supported by the Science and Technology Planning Social Development Project of Zhenjiang City (SH2020030).

Conflict of Interest

The authors declare no conflict of interest.

Supplementary Material

Supplementary material associated with this article can be found, in the online version, at https://doi.org/10.59958/hsf.5925.

References

[1] Ross R. Atherosclerosis–an inflammatory disease. The New England Journal of Medicine. 1999; 340: 115–126.

[2] Gallino A, Aboyans V, Diehm C, Cosentino F, Stricker H, Falk E, *et al*. Non-coronary atherosclerosis. European Heart Journal. 2014; 35: 1112–1119.

[3] Libby P. The changing landscape of atherosclerosis. Nature. 2021; 592: 524–533.

[4] Gisterå A, Hansson GK. The immunology of atherosclerosis. Nature Reviews. Nephrology. 2017; 13: 368–380.

[5] Jukema RA, Ahmed TAN, Tardif JC. Does low-density lipoprotein cholesterol induce inflammation? If so, does it matter? Current insights and future perspectives for novel therapies. BMC Medicine. 2019; 17: 197.

[6] Bäck M, Yurdagul A, Jr, Tabas I, Öörni K, Kovanen PT. Inflammation and its resolution in atherosclerosis: mediators and therapeutic opportunities. Nature Reviews. Cardiology. 2019; 16: 389–406.

[7] Torzewski M. The Initial Human Atherosclerotic Lesion and Lipoprotein Modification-A Deep Connection. International Journal of Molecular Sciences. 2021; 22: 11488.

[8] Wei Y, Corbalán-Campos J, Gurung R, Natarelli L, Zhu M, Exner N, *et al*. Dicer in Macrophages Prevents Atherosclerosis by Promoting Mitochondrial Oxidative Metabolism. Circulation. 2018; 138: 2007–2020.

[9] Kubo T, Maehara A, Mintz GS, Doi H, Tsujita K, Choi SY, *et al*. The dynamic nature of coronary artery lesion morphology assessed by serial virtual histology intravascular ultrasound tissue characterization. Journal of the American College of Cardiology. 2010; 55: 1590–1597.

[10] Tabas I, Bornfeldt KE. Intracellular and Intercellular Aspects of Macrophage Immunometabolism in Atherosclerosis. Circulation Research. 2020; 126: 1209–1227.

[11] Röszer T. Transcriptional control of apoptotic cell clearance by macrophage nuclear receptors. Apoptosis: an International Journal on Programmed Cell Death. 2017; 22: 284–294.

[12] Tabas I, Bornfeldt KE. Macrophage Phenotype and Function in Different Stages of Atherosclerosis. Circulation Research. 2016; 118: 653–667.

[13] Malandrino MI, Fucho R, Weber M, Calderon-Dominguez M, Mir JF, Valcarcel L, *et al*. Enhanced fatty acid oxidation in adipocytes and macrophages reduces lipid-induced triglyceride accumulation and inflammation. American Journal of Physiology. Endocrinology and Metabolism. 2015; 308: E756–E769.

[14] Björnheden T, Bondjers G. Oxygen consumption in aortic tissue from rabbits with diet-induced atherosclerosis. Arteriosclerosis. 1987; 7: 238–247.

[15] Roy P, Orecchioni M, Ley K. How the immune system shapes atherosclerosis: roles of innate and adaptive immunity. Nature Reviews of Immunology. 2022; 22: 251–265.

[16] Zhong Z, Wu H, Zhang Q, Zhong W, Zhao P. Characteristics of T cell receptor repertoires of patients with acute myocardial infarction through high-throughput sequencing. Journal of Translational Medicine. 2019; 17: 21.

[17] Ketelhuth DFJ, Hansson GK. Adaptive Response of T and B Cells in Atherosclerosis. Circulation Research. 2016; 118: 668–678.

[18] Libby P, Hansson GK. From Focal Lipid Storage to Systemic Inflammation: JACC Review Topic of the Week. Journal of the American College of Cardiology. 2019; 74: 1594–1607.
[19] Kyaw T, Tay C, Krishnamurthi S, Kanellakis P, Agrotis A, Tipping P, *et al*. B1a B lymphocytes are atheroprotective by secreting natural IgM that increases IgM deposits and reduces necrotic cores in atherosclerotic lesions. Circulation Research. 2011; 109: 830–840.
[20] Taminau J, Meganck S, Lazar C, Steenhoff D, Coletta A, Molter C, *et al*. Unlocking the potential of publicly available microarray data using inSilicoDb and inSilicoMerging R/Bioconductor packages. BMC Bioinformatics. 2012; 13: 335.
[21] Johnson WE, Li C, Rabinovic A. Adjusting batch effects in microarray expression data using empirical Bayes methods. Biostatistics. 2007; 8: 118–127.
[22] Birsoy K, Wang T, Chen WW, Freinkman E, Abu-Remaileh M, Sabatini DM. An Essential Role of the Mitochondrial Electron Transport Chain in Cell Proliferation Is to Enable Aspartate Synthesis. Cell. 2015; 162: 540–551.
[23] Tsvetkov P, Coy S, Petrova B, Dreishpoon M, Verma A, Abdusamad M, *et al*. Copper induces cell death by targeting lipoylated TCA cycle proteins. Science. 2022; 375: 1254–1261.
[24] Liberzon A, Subramanian A, Pinchback R, Thorvaldsdóttir H, Tamayo P, Mesirov JP. Molecular signatures database (MSigDB) 3.0. Bioinformatics. 2011; 27: 1739–1740.
[25] Lai D, Tan L, Zuo X, Liu D, Jiao D, Wan G, *et al*. Prognostic Ferroptosis-Related lncRNA Signatures Associated With Immunotherapy and Chemotherapy Responses in Patients With Stomach Cancer. Frontiers in Genetics. 2022; 12: 798612.
[26] Ru B, Wong CN, Tong Y, Zhong JY, Zhong SSW, Wu WC, *et al*. TISIDB: an integrated repository portal for tumor-immune system interactions. Bioinformatics. 2019; 35: 4200–4202.
[27] Muhammad K, Ayoub MA, Iratni R. Vascular Inflammation in Cardiovascular Disease: Is Immune System Protective or Bystander? Current Pharmaceutical Design. 2021; 27: 2141–2150.
[28] Lacy M, Atzler D, Liu R, de Winther M, Weber C, Lutgens E. Interactions between dyslipidemia and the immune system and their relevance as putative therapeutic targets in atherosclerosis. Pharmacology & Therapeutics. 2019; 193: 50–62.
[29] Koskimäki J, Girard R, Li Y, Saadat L, Zeineddine HA, Lightle R, *et al*. Comprehensive transcriptome analysis of cerebral cavernous malformation across multiple species and genotypes. JCI Insight. 2019; 4: e126167.
[30] Chmielowski RA, Abdelhamid DS, Faig JJ, Petersen LK, Gardner CR, Uhrich KE, *et al*. Athero-inflammatory nanotherapeutics: Ferulic acid-based poly(anhydride-ester) nanoparticles attenuate foam cell formation by regulating macrophage lipogenesis and reactive oxygen species generation. Acta Biomaterialia. 2017; 57: 85–94.
[31] Cunrath O, Bumann D. Host resistance factor SLC11A1 restricts *Salmonella* growth through magnesium deprivation. Science. 2019; 366: 995–999.
[32] Xu H, Zhang A, Fang C, Zhu Q, Wang W, Liu Y, *et al*. SLC11A1 as a stratification indicator for immunotherapy or chemotherapy in patients with glioma. Frontiers in Immunology. 2022; 13: 980378.
[33] Ma PY, Tan JE, Hee EW, Yong DWX, Heng YS, Low WX, *et al*. Human Genetic Variation Influences Enteric Fever Progression. Cells. 2021; 10: 345.
[34] Haschka D, Hoffmann A, Weiss G. Iron in immune cell function and host defense. Seminars in Cell & Developmental Biology. 2021; 115: 27–36.
[35] Fu D, Zhang Z, Wallrad L, Wang Z, Höller S, Ju C, *et al*. Ca^{2+}-dependent phosphorylation of NRAMP1 by CPK21 and CPK23 facilitates manganese uptake and homeostasis in *Arabidopsis*. Proceedings of the National Academy of Sciences of the United States of America. 2022; 119: e2204574119.
[36] Deng M, Chen Z, Tan J, Liu H. Down-regulation of SLC35C1 induces colon cancer through over-activating Wnt pathway. Journal of Cellular and Molecular Medicine. 2020; 24: 3079–3090.
[37] Cooper N, Li YT, Möller A, Schulz-Weidner N, Sachs UJ, Wagner F, *et al*. Incidental diagnosis of leukocyte adhesion deficiency type II following ABO typing. Clinical Immunology. 2020; 221: 108599.
[38] Chen L, Zhang J, Yang X, Liu Y, Deng X, Yu C. Lysophosphatidic acid decreased macrophage foam cell migration correlated with downregulation of fucosyltransferase 8 via HNF1α. Atherosclerosis. 2019; 290: 19–30.
[39] Xue S, Su Z, Liu D. Immunometabolism and immune response regulate macrophage function in atherosclerosis. Ageing Research Reviews. 2023; 90: 101993.
[40] Zhao Q, Wang Z, Meyers AK, Madenspacher J, Zabalawi M, Zhang Q, *et al*. Hematopoietic Cell-Specific SLC37A2 Deficiency Accelerates Atherosclerosis in LDL Receptor-Deficient Mice. Frontiers in Cardiovascular Medicine. 2021; 8: 777098.
[41] Fang Y, Liu W, Tang Z, Ji X, Zhou Y, Song S, *et al*. Monocarboxylate transporter 4 inhibition potentiates hepatocellular carcinoma immunotherapy through enhancing T cell infiltration and immune attack. Hepatology. 2023; 77: 109–123.
[42] Payen VL, Mina E, Van Hée VF, Porporato PE, Sonveaux P. Monocarboxylate transporters in cancer. Molecular Metabolism. 2020; 33: 48–66.
[43] Cluntun AA, Badolia R, Lettlova S, Parnell KM, Shankar TS, Diakos NA, *et al*. The pyruvate-lactate axis modulates cardiac hypertrophy and heart failure. Cell Metabolism. 2021; 33: 629–648.e10.
[44] Ouimet M, Franklin V, Mak E, Liao X, Tabas I, Marcel YL. Autophagy regulates cholesterol efflux from macrophage foam cells via lysosomal acid lipase. Cell Metabolism. 2011; 13: 655–667.
[45] Povero D, Johnson SM, Liu J. Hypoxia, hypoxia-inducible gene 2 (HIG2)/HILPDA, and intracellular lipolysis in cancer. Cancer Letters. 2020; 493: 71–79.
[46] Zhang W, Xu L, Zhu L, Liu Y, Yang S, Zhao M. Lipid Droplets, the Central Hub Integrating Cell Metabolism and the Immune System. Frontiers in Physiology. 2021; 12: 746749.
[47] Liu R, Lee JH, Li J, Yu R, Tan L, Xia Y, *et al*. Choline kinase alpha 2 acts as a protein kinase to promote lipolysis of lipid droplets. Molecular Cell. 2021; 81: 2722–2735.e9.
[48] Ma Q, Meng Z, Meng Y, Liu R, Lu Z. A moonlighting function of choline kinase alpha 2 in the initiation of lipid droplet lipolysis in cancer cells. Cancer Communications. 2021; 41: 933–936.
[49] Poznyak AV, Bharadwaj D, Prasad G, Grechko AV, Sazonova MA, Orekhov AN. Anti-Inflammatory Therapy for Atherosclerosis: Focusing on Cytokines. International Journal of Molecular Sciences. 2021; 22: 7061.
[50] Tam LS, Kitas GD, González-Gay MA. Can suppression of inflammation by anti-TNF prevent progression of subclinical atherosclerosis in inflammatory arthritis? Rheumatology. 2014; 53: 1108-1119.
[51] Biros E, Moran CS, Maguire J, Holliday E, Levi C, Golledge J. Upregulation of arylsulfatase B in carotid atherosclerosis is associated with symptoms of cerebral embolization. Scientific Reports. 2017; 7: 4338.
[52] Das S, Ray R, Snehlata, Das N, Srivastava LM. Effect of ascorbic acid on prevention of hypercholesterolemia induced atherosclerosis. Molecular and Cellular Biochemistry. 2006; 285: 143–147.
[53] Moser MA, Chun OK. Vitamin C and Heart Health: A Review Based on Findings from Epidemiologic Studies. International Journal of Molecular Sciences. 2016; 17: 1328.
[54] van Tuijl J, Joosten LAB, Netea MG, Bekkering S, Riksen NP. Immunometabolism orchestrates training of innate immunity in atherosclerosis. Cardiovascular Research. 2019; 115: 1416–

1424.
[55] Zhang SJ, Li ZH, Zhang YD, Chen J, Li Y, Wu FQ, *et al*. Ketone Body 3-Hydroxybutyrate Ameliorates Atherosclerosis via Receptor Gpr109a-Mediated Calcium Influx. Advanced Science. 2021; 8: 2003410.
[56] Billingham LK, Stoolman JS, Vasan K, Rodriguez AE, Poor TA, Szibor M, *et al*. Mitochondrial electron transport chain is necessary for NLRP3 inflammasome activation. Nature Immunology. 2022; 23: 692–704.
[57] Barra NG, Henriksbo BD, Anhê FF, Schertzer JD. The NLRP3 inflammasome regulates adipose tissue metabolism. The Biochemical Journal. 2020; 477: 1089–1107.
[58] Meyers AK, Zhu X. The NLRP3 Inflammasome: Metabolic Regulation and Contribution to Inflammaging. Cells. 2020; 9: 1808.
[59] Poznyak AV, Bharadwaj D, Prasad G, Grechko AV, Sazonova MA, Orekhov AN. Renin-Angiotensin System in Pathogenesis of Atherosclerosis and Treatment of CVD. International Journal of Molecular Sciences. 2021; 22: 6702.
[60] Sluimer JC, Gasc JM, Hamming I, van Goor H, Michaud A, van den Akker LH, *et al*. Angiotensin-converting enzyme 2 (ACE2) expression and activity in human carotid atherosclerotic lesions. The Journal of Pathology. 2008; 215: 273–279.
[61] Batlle M, Roig E, Perez-Villa F, Lario S, Cejudo-Martin P, García-Pras E, *et al*. Increased expression of the renin-angiotensin system and mast cell density but not of angiotensin-converting enzyme II in late stages of human heart failure. The Journal of Heart and Lung Transplantation. 2006; 25: 1117–1125.
[62] Fernandez DM, Rahman AH, Fernandez NF, Chudnovskiy A, Amir EAD, Amadori L, *et al*. Single-cell immune landscape of human atherosclerotic plaques. Nature Medicine. 2019; 25: 1576–1588.
[63] Sage AP, Tsiantoulas D, Binder CJ, Mallat Z. The role of B cells in atherosclerosis. Nature Reviews. Cardiology. 2019; 16: 180–196.
[64] Foks AC, Ran IA, Wasserman L, Frodermann V, Ter Borg MND, de Jager SCA, *et al*. T-cell immunoglobulin and mucin domain 3 acts as a negative regulator of atherosclerosis. Arteriosclerosis, Thrombosis, and Vascular Biology. 2013; 33: 2558–2565.
[65] Lian C, Wang Z, Qiu J, Jiang B, Lv J, He R, *et al*. TIM 3 inhibits PDGF BB induced atherogenic responses in human artery vascular smooth muscle cells. Molecular Medicine Reports. 2020; 22: 886–894.
[66] Cong Y, Wang X, Wang S, Qiao G, Li Y, Cao J, *et al*. Tim-3 promotes tube formation and decreases tight junction formation in vascular endothelial cells. Bioscience Reports. 2020; 40: BSR20202130.
[67] Mulholland M, Kritikou E, Katra P, Nilsson J, Björkbacka H, Lichtman AH, *et al*. LAG3 Regulates T Cell Activation and Plaque Infiltration in Atherosclerotic Mice. JACC. CardioOncology. 2022; 4: 635–645.
[68] Yousif LI, Tanja AA, de Boer RA, Teske AJ, Meijers WC. The role of immune checkpoints in cardiovascular disease. Frontiers in Pharmacology. 2022; 13: 989431.
[69] Minami H, Nagaharu K, Nakamori Y, Ohishi K, Shimojo N, Kageyama Y, *et al*. CXCL12-CXCR4 Axis Is Required for Contact-Mediated Human B Lymphoid and Plasmacytoid Dendritic Cell Differentiation but Not T Lymphoid Generation. Journal of Immunology. 2017; 199: 2343–2355.
[70] Wang J, Xie J, Wang D, Han X, Chen M, Shi G, *et al*. CXCR4^{high} megakaryocytes regulate host-defense immunity against bacterial pathogens. eLife. 2022; 11: e78662.
[71] Georgakis MK, Bernhagen J, Heitman LH, Weber C, Dichgans M. Targeting the CCL2-CCR2 axis for atheroprotection. European Heart Journal. 2022; 43: 1799–1808.
[72] Jongstra-Bilen J, Tai K, Althagafi MG, Siu A, Scipione CA, Karim S, *et al*. Role of myeloid-derived chemokine CCL5/RANTES at an early stage of atherosclerosis. Journal of Molecular and Cellular Cardiology. 2021; 156: 69–78.
[73] Apostolakis S, Spandidos D. Chemokines and atherosclerosis: focus on the CX3CL1/CX3CR1 pathway. Acta Pharmacologica Sinica. 2013; 34: 1251–1256.
[74] de Jager SCA, Bongaerts BWC, Weber M, Kraaijeveld AO, Rousch M, Dimmeler S, *et al*. Chemokines CCL3/MIP1α, CCL5/RANTES and CCL18/PARC are independent risk predictors of short-term mortality in patients with acute coronary syndromes. PLoS ONE. 2012; 7: e45804.
[75] De Sutter J, Struyf S, Van de Veire NR, Philippé J, De Buyzere M, Van Damme J. Cardiovascular determinants and prognostic significance of CC Chemokine Ligand-18 (CCL18/PARC) in patients with stable coronary artery disease. Journal of Molecular and Cellular Cardiology. 2010; 49: 894–896.
[76] Shi C, Pamer EG. Monocyte recruitment during infection and inflammation. Nature Reviews. Immunology. 2011; 11: 762–774.
[77] Ghattas A, Griffiths HR, Devitt A, Lip GYH, Shantsila E. Monocytes in coronary artery disease and atherosclerosis: where are we now? Journal of the American College of Cardiology. 2013; 62: 1541–1551.
[78] Gisterå A, Klement ML, Polyzos KA, Mailer RKW, Duhlin A, Karlsson MCI, *et al*. Low-Density Lipoprotein-Reactive T Cells Regulate Plasma Cholesterol Levels and Development of Atherosclerosis in Humanized Hypercholesterolemic Mice. Circulation. 2018; 138: 2513–2526.
[79] Backteman K, Andersson C, Dahlin LG, Ernerudh J, Jonasson L. Lymphocyte subpopulations in lymph nodes and peripheral blood: a comparison between patients with stable angina and acute coronary syndrome. PLoS ONE. 2012; 7: e32691.
[80] Podolec J, Niewiara L, Skiba D, Siedlinski M, Baran J, Komar M, *et al*. Higher levels of circulating naïve CD8$^+$CD45RA$^+$ cells are associated with lower extent of coronary atherosclerosis and vascular dysfunction. International Journal of Cardiology. 2018; 259: 26–30.
[81] Huang SCC, Pearce EJ. For macrophages, Ndufs is enough. Immunity. 2014; 41: 351–353.
[82] Jin Z, Wei W, Yang M, Du Y, Wan Y. Mitochondrial complex I activity suppresses inflammation and enhances bone resorption by shifting macrophage-osteoclast polarization. Cell Metabolism. 2014; 20: 483–498.
[83] Schirris TJJ, Rossell S, de Haas R, Frambach SJCM, Hoogstraten CA, Renkema GH, *et al*. Stimulation of cholesterol biosynthesis in mitochondrial complex I-deficiency lowers reductive stress and improves motor function and survival in mice. Biochimica et Biophysica Acta. Molecular Basis of Disease. 2021; 1867: 166062.
[84] Li M, Xin S, Gu R, Zheng L, Hu J, Zhang R, *et al*. Novel Diagnostic Biomarkers Related to Oxidative Stress and Macrophage Ferroptosis in Atherosclerosis. Oxidative Medicine and Cellular Longevity. 2022; 2022: 8917947.
[85] Zhao L, Lv F, Zheng Y, Yan L, Cao X. Characterization of an Aging-Based Diagnostic Gene Signature and Molecular Subtypes With Diverse Immune Infiltrations in Atherosclerosis. Frontiers in Molecular Biosciences. 2022; 8: 792540.